Control through Monomer Placement of Surface Properties and Morphology of Fluoromethacrylate Copolymers

Ao Chen,[1] Idriss Blakey,[1,2] Kevin S. Jack,[3] Andrew K. Whittaker[1,2,4] and Hui Peng[1,4*]

[1]Australian Institute for Bioengineering and Nanotechnology, The University of Queensland, Brisbane Qld 4072
[2]Centre for Advanced Imaging, The University of Queensland, Brisbane Qld 4072
[3]Centre for Microscopy and Microanalysis, The University of Queensland, Brisbane Qld 4072
[4]Australian Research Council Centre of Excellence for Convergent Bio-Nano Science and Technology
Correspondence to: Dr Hui Peng (E-mail: h.peng@uq.edu.au)

((Additional Supporting Information may be found in the online version of this article.))

ABSTRACT

The arrangement of monomers and morphology of fluorinated copolymers of methyl methacrylate was found to be important for controlling the surface energy of the materials when formed into thin films. Novel copolymers of methyl methacrylate (MMA) and 2,2,3,3,4,4,4-heptafluorobutyl methacrylate (F3MA) were prepared with different monomer placement, namely statistical and block arrangements of the monomer units. The surface energies decreased with increasing incorporation of F3MA, in a manner consistent with previous reports for similar copolymers, however the surface energies of the block copolymers were consistently lower than the statistical copolymers. This was interpreted as arising from conformational restriction of presentation of the fluoromonomers to the surface in the statistical copolymers, and formation of phase-separated domains at the surface of the block copolymers. The morphology of the block copolymers was confirmed by SAXS measurements, which allowed calculation of a solubility parameter for the fluorinated segments. The results have implications for the design of more environmentally acceptable materials with ultra-low surface energies.

KEYWORDS: fluoropolymers; low surface energy; phase separation; block copolymers; reversible addition fragmentation chain transfer (RAFT), SAXS

INTRODUCTION

The tendency for a liquid to spread and wet a surface of a polymeric substrate is determined by the balance of forces of adhesion between the liquid and the substrate, and the forces of cohesion driving the liquid into a form with a minimum surface energy, i.e. a sphere. Spreading continues until the adhesion forces are matched by the combined surface forces. As we know, the forces of adhesion are determined by the magnitude of the non-covalent or van der Waal's interactions in the system. For a polar liquid such as water these are dominated by the presence of permanent dipoles, and so spreading of water is facilitated by the presence of functionalities with similar polarity within the substrate. Such polar substrates have high surface energies, as a result of the disruption of these strong forces at the material-air interface. On the contrary, it has been known for many years that the incorporation of fluorinated segments into polymers imparts low surface energy, and thus water tends to dewet extensively on planar fluorinated surfaces. These properties have led to many important applications for fluoropolymers, for example

in engineering, health and the electronics industries. Thus, by way of illustration, the low forces of adhesion to fluoropolymers have been exploited in anti-fouling surfaces, to impart resistance to accumulation of proteins in medical devices, and of microbes to surfaces. For example, in 1992, Lindner demonstrated the ability of fluoroalkyl polymethacrylates and polyacrylates to resist marine biofouling.[1] More recent research has shown that crosslinked fluorinated polymer coatings can be highly resistant against marine organisms such as algae. Networks prepared from poly(1H,1H,2H,2H-heptadecafluorodecyl acrylate)-co-poly(acrylic acid) and poly(2-isopropenyl-2-oxazoline)-co-poly(methyl methacrylate) show good marine biofouling and release behaviour.[2] In another study, a series of photocrosslinked terpolymers of perfluoropolyether grafted to alkyl methacrylamide monomers and glycidyl methacrylate exhibited promising antibiofouling behaviour against marine algae of the species Ulva.[3]

In addition to marine organisms, fluorinated polymer coatings also possess properties of excellent resistance against adsorption by proteins, as illustrated in the work by Dimitriou et al. who used thiol-ene chemistry to attach 1H,1H,2H,2H-perfluorooctanethiol to polystyrene-*block*-poly[(ethylene oxide)-*co*-(allyl glycidyl ether)], and demonstrated resistance to adhesion by bovine serum albumin.[4] Since adhesion of proteins is considered a prerequisite for attachment of bacteria, fluorinated polymers show promise as components of antimicrobial coatings for use in the biomedical field. However, longer (>C6) perfluoroalkyl chains have been shown to be persistent in the environment and undergo bioaccumulation in some aquatic species.[5,6] Unfortunately, this limits the ability to incorporate longer perfluoroalkyl chains in commercial coatings. On the other hand, shorter perfluorinated alkyl chains, such as those studied here, have a much lower degree of bioconcentration.[7] However, the surface energies of statistical copolymers with shorter perfluoroalkyl chains have been shown to be higher than their longer analogues, which means they are less effective in repelling water.[8]

Another important property of fluorinated components is their strong incompatibility with hydrophilic and non-fluorous hydrophobic species. In polymers this can lead to formation of phase-separated structures in the bulk phase and when appropriate conditions are satisfied block copolymers where one block is fluorous can result in ordered nanoscale morphologies. In a detailed study,[9-11] Hillmyer and colleagues investigated the phase behaviour of polystyrene-*block*-polyisoprene (PS-*b*-PI) and polystyrene-*block*-poly(1,2-polybutadiene) (PS-*b*-PBD) before and after progressive fluorination of the elastomeric blocks. It was found that the incompatibility of the two blocks increased after fluorination, consistent with an increase in the Flory-Huggins interaction parameter (χ). In another study, the relationship between fraction of the fluorinated block (PF) and surface structure of asymmetrical polystyrene-*block*-poly[4-(perfluorooctylpropyloxy)styrene] (PS-*b*-PF) was investigated in detail by Yokoyama *et al*.[12] It was found that the weight fraction of the PF block, f_{PF}, significantly affects the conformation of the fluorinated side chains at the surface. In later work, the same authors used annealing in supercritical CO_2 to lower the interaction parameter of PS-*b*-PF to improve the inter-mixing of the chains and increase the rate of diffusion of the polymer.[13] Coatings having thicker domain sizes and lower surface energies were achieved under such conditions.

Despite such achievements, these studies demonstrate that a detailed understanding of both the surface and bulk properties is

required for a complete appreciation of the behaviour of partly fluorinated polymers, and of their potential applications.

In this current study we report the synthesis of novel copolymers of a partly-fluorinated methacrylate monomer and methyl methacrylate (MMA), and characterize both the surface properties and the bulk morphologies of the polymers. Importantly the fluoro-methacrylate contains short fluoroalkyl side chains (n=3) and therefore is more environmentally acceptable than polymers containing longer fluorinated chains. To determine the effect of polymer topology, both block copolymers and polymers in which the placement of the monomers is determined by the statistics of copolymerisation are examined. As expected the fluorinated segments have a strong tendency to aggregate at the air-polymer interface, however, the extent to which this occurs depends on the composition and topology of the copolymers. Detailed synchrotron-based small-angle X-ray scattering measurements have revealed the phase behaviour of the block copolymers and allowed an estimation of the solubility parameter of the fluorinated segments and confirmation of the phase behaviour of the copolymers. The work provides additional insights into effect of monomer placement on phase behaviour of partly-fluorinated copolymers.

EXPERIMENTAL

Materials

All chemicals were purchased from Sigma-Aldrich unless otherwise stated. Methyl methacrylate (MMA) and 2,2,3,3,4,4,4-heptafluorobutyl methacrylate (F3MA) were passed through basic alumina columns to remove inhibitors prior to use. 2,2'-Azobis(2-methylpropionitrile) (AIBN) was recrystallized twice from methanol before use. The RAFT agent, 4-cyano-4-(phenylcarbonothioylthio) pentanoic acid (CPADB), was synthesized according to a previously reported procedure.[14] Dried toluene and tetrahydrofuran (THF) were obtained oxygen- and moisture-free using a purification unit under an inert nitrogen environment (MBraun Solvent Purification System Auto-5).

Characterisation

^{1}H NMR spectra of the polymer intermediates were measured in $CDCl_3$ on a Bruker Avance 500 MHz spectrometer with a TXI probe at 298 K. A 90° pulse of 10 µs and a repetition delay (D1) of 10 s were used in all cases. The spectrum width was 8 kHz, and 32 k data points were collected.

Size exclusion chromatography (SEC) measurements were performed using a Waters Alliance 2690 Separations Module equipped with an autosampler, column heater, differential refractive index detector, and a Photodiode Array (PDA) connected in series. HPLC-grade tetrahydrofuran was used as eluent at a flow rate of 1 mL/min. The columns consisted of three 7.8 × 300 mm Waters Styragel SEC columns connected in series, comprising two linear UltraStyragel and one Styragel HR3 columns. Polystyrene standards ranging from 517 to 2×10^6 g mol^{-1} were used for calibration.

UV-Vis measurements were conducted on a Varian UV-Vis Cary 4000 spectrophotometer. Solutions with a fixed polymer concentration of 10 mg/mL were prepared in THF and the absorption spectra were recorded over a wavelength range of 200 nm to 800 nm.

Static contact angles (CA) were measured using a Data Physics Instruments Optical Contact Angle Series 5 (OCA 5) goniometer. The contact angles reported here were measured by the addition of a 5 µL drop of either water or diiodomethane at five

different locations for each thin film. Contact angles were measured before and after annealing (see below for annealing conditions) and the values were in agreement to within 1.6 erg/cm^2.

XPS measurements were performed using a Kratos Axis ULTRA spectrometer (Kratos Analytical, Manchester, U.K.) with a 165 mm hemispherical electron-energy analyzer and monochromatic Al Kα X-ray source (1486.6 eV) operating at 300 W (15 kV, 20 mA). Survey (wide) spectra were acquired using an analyzer pass energy of 160 eV and were carried out over a 1200−0 eV binding energy range with 1.0 eV steps and a 100 ms dwell time. High-resolution spectra were acquired at an analyzer pass energy of 20 eV with 0.1 eV steps and a 250 ms dwell time, with no charge neutralisation. The XPS spectra were analyzed using CasaXPS version 2.3.12 software. A small shift of the aliphatic carbon peak in the C1s spectrum was observed, and so the peak was rescaled to 285 eV to compensate for charging effects.

Small Angle X-ray Scattering (SAXS) experiments were performed on the SAXS/WAXS beam-line at the Australian Synchrotron, Clayton, Australia. The beam-line was configured with an X-ray wavelength of λ = 1.127 Å and was focused to a 235 µm horizontal × 140 µm vertical spot. Two dimensional scattering patterns were recorded on a Dectris - Pilatus 1M detector at a sample-to-detector distance of 3341 mm; calibrated using a silver behenate standard. The scattering patterns were then azimuthally integrated to give one-dimensional scattering data as intensity (I) versus wave vector (q), where $q = 4\pi \sin(\vartheta/2)/\lambda$, and ϑ is the scattering angle.

Synthesis of poly(methyl methacrylate)-block-poly(2,2,3,3,4,4,4-heptafluorobutyl methacrylate) (poly(MMA-*block*-F3MA))

The poly(methyl methacrylate) (PMMA) macro-chain transfer agent (macro-CTA) was synthesized according to the following procedure: MMA (1.87 g, 18.7 mmol), 4-cyano-4-(phenylcarbonothioylthio) pentanoic acid (CPADB) (0.104 g, 0.37 mmol) and AIBN (12.3 mg, 0.07 mmol) were dissolved in 3 mL of toluene in a 25 mL round bottom flask equipped with a magnetic stirrer bar and sealed with a rubber septum. The solution was purged with nitrogen for 15 min in an ice bath, followed by being immersed in an oil bath thermostated at 70 °C. After 5 h, the polymerisation was quenched by placing the flask in an ice bath and exposing to air for 5 min. The crude polymer solution was precipitated into methanol and washed three times. A pink powder was obtained after vacuum drying (1.6 g, yield: 86%). The molecular weights of the final product were determined by both size exclusion chromatography (SEC) and ^{1}H NMR. M_n = 3340, $Đ_M$= 1.12, degree of polymerisation (DP) = 33. Similar procedures were applied to prepare block copolymers from the PMMA-CTA; by varying the ratio of F3MA to PMMA-CTA, block copolymers poly(MMA-*block*-F3MA) with different chain lengths were prepared. The RAFT end group was removed by reaction with an excess of AIBN.[15] Polymer, AIBN and THF were added in a 25 mL round bottom flask equipped with a magnetic stirrer bar and sealed with a rubber septum. As an example, for removal of the end group from poly(MMA_{33}-*block*-$F3MA_{22}$), 0.5 g of polymer (5.73×10^{-5} mol) and 0.188 g of AIBN (0.00115 mol) were added to 10 mL of THF. The solution was purged with nitrogen for 15 min in an ice bath, followed by being immersed in an oil bath maintained at 80 °C overnight. The crude polymer solution was precipitated into cold hexane and washed three times. A white powder was obtained. The ratio of AIBN to RAFT end group was set to 20:1.

Synthesis of poly(methyl methacrylate)-*statistic*-poly(2,2,3,3,4,4,4-heptafluorobutyl methacrylate) (poly(MMA-*stat*-F3MA))

Statistical copolymers of MMA and F3MA were prepared by a similar procedure to that used to prepare PMMA. MMA and F3MA were added together at the beginning of the reaction, and by varying their ratio to the CPADB RAFT agent, statistical copolymers poly(MMA-*stat*-F3MA) with different chain lengths were made. The RAFT end group of poly(MMA-*stat*-F3MA) was removed by applying a 20:1 ratio of AIBN to the RAFT end group, as described above.

Preparation of polymeric films

Thin films of various polymers were prepared by spin-coating 1 wt. % of polymer in propylene glycol methyl ether acetate (PGMEA) onto silicon wafers (300 rpm for 5 s, followed by 3000 rpm for 60 s). The thickness of the film was controlled by modifying the concentration of the block copolymer solutions and by adjusting the spin speed of the spin coater. All copolymers films were annealed at 150 °C in a vacuum oven (600 mm Hg) for 4 h. This is well above the glass temperatures of all polymers. The films had a thickness of the order of 85-100 nm, as determined by profilometry.

Preparation of samples for SAXS analysis

Samples were placed in an aluminium plate that had been drilled with an array of 12 × 8 holes in a similar format to 96 well cell culture plates. One side of the wells was covered with Kapton tape. Each block copolymer was dissolved in THF at a concentration of 5 wt. %. The solution was then filtered through a 0.45 µm filter and loaded into the well. All samples were dried at room temperature under standard pressure overnight to fully evaporate the solvent and were annealed at 150 °C. After slowly cooling down to room temperature, the wells were covered with another piece of Kapton tape.

RESULTS AND DISCUSSION

In this study, block and statistical copolymers, poly(MMA-*block*-F3MA) and poly(MMA-*stat*-F3MA) were prepared by RAFT polymerisation and their bulk and surface properties examined in detail. The potential for application of these polymers in a number of fields will be discussed.

Synthesis of poly(MMA-*block*-F3MA) and (poly(MMA-*stat*-F3MA)

A series of block and statistical copolymers of MMA and F3MA were prepared by RAFT polymerisation using CPADB as a chain transfer agent. The approach to the synthesis of the block copolymers is schematically summarized in Scheme 1 below and the synthesis of the statistic copolymers in shown in the Supporting Information Scheme S1. The compositions of the block copolymers ranged from 40 to 77 mole % MMA. Statistical copolymers (24-82 mole % MMA) were prepared by polymerisation of the appropriate monomer mixture in a single step. The phenyl dithioester end group of the polymer was cleaved by heating within a solution containing 20 equivalents of AIBN, to remove any influence the end groups may have on the bulk ordering or surface properties.[15]

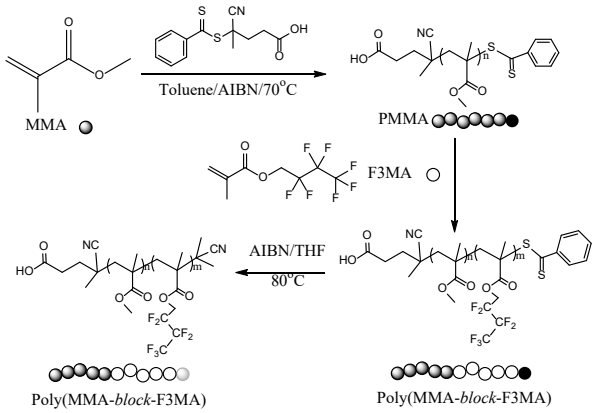

Scheme 1 Schematic illustration of the synthesis of the block polymers.

A detailed study of the structure of the copolymers was conducted using solution-based techniques, such as ^{1}H NMR and size exclusion chromatography (SEC). A typical ^{1}H NMR spectrum of a block copolymer (in this case of composition poly(MMA$_{33}$-*block*-F3MA$_{39}$) is shown below in Figure 1, and additional spectra are included in the Supporting Information Figure S1. The spectrum shows characteristic peaks from 0.8-1.2 due to the protons of the alpha-methyl groups, split by tacticity and sequence effects.[16] The resonances from the main-chain methylene protons lie from 1.2 to 2.2 ppm. The compositions of the copolymers were determined by integration of the peaks at 3.58 ppm and 4.39 ppm due to protons of the methyl and methylene groups of MMA and F3MA repeat units, respectively. The results are summarized in Table 1. As discussed above the RAFT end group was removed by reaction of the polymer in solution with an excess of AIBN.[15] The UV-visible spectrum after reaction with AIBN (Figure 2) confirms the complete removal of the aromatic RAFT agent.

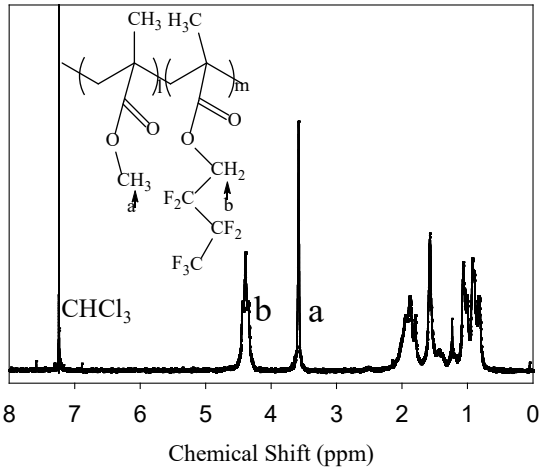

Figure 1 ^{1}H NMR spectrum of poly(MMA$_{33}$-*block*-F3MA$_{39}$), with assignments to the spectrum. Peak assignments are discussed in the text.

Table 1 Molecular characteristics of the fluorine-containing copolymers.

Polymer	M_n (^{1}H NMR)	DP (^{1}H NMR) [MMA]:[F3MA]	*Mole Fn.* MMA	M_n (SEC)	$Đ_M$
PMMA	3500	35:0	1.00	3300	1.12
PF3MA	14200	0:53	0.00	12600	1.10
poly(MMA-*block*-F3MA)	6700	37:11	0.77	7100	1.12
	9200	33:22	0.60	8800	1.03
	10700	37:26	0.59	8900	1.11
	13800	33:39	0.46	12700	1.02
	16400	33:49	0.40	15400	1.06
poly(MMA-*stat*-F3MA)	13000	82:18	0.82	10100	1.17
	12500	69:21	0.77	11200	1.18
	11200	58:20	0.74	11200	1.06
	12300	32:34	0.48	12300	1.06
	14400	15:48	0.24	14300	1.07

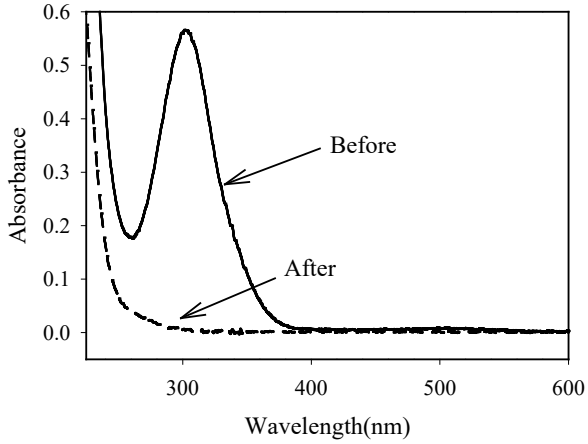

Figure 2 UV-visible spectra of a typical block copolymer of MMA and F3MA before (solid line) and after (dashed line) removal of the RAFT end group.

The molecular weights (polystyrene equivalents) of the copolymers were determined by size exclusion chromatography with tetrahydrofuran as eluent. In all cases the molar mass dispersity ($Đ_M$) was below 1.2 and usually below 1.1, indicating good control of the RAFT polymerisation. Representative SEC traces are shown in the Supporting Information Figure S2.

Surface properties of statistical and block copolymers

The incorporation of fluorinated segments into polymer structures is well known to

lead to preferential accumulation of these units at the polymer-air interface, which minimises the surface free energy. This phenomenon has been exploited not only to prepare materials of low surface energy, but also to drive specific functional groups to the polymer-air interface.[17-20] A convenient method for measuring atomic composition of the surface of a material is X-ray photoelectron spectroscopy (XPS). The fluorine contents of the surfaces of the polymer films measured by XPS are listed in Table 2. Figure 3 shows a plot of the surface content of fluorine atoms as a function of the bulk fluorine content calculated from the structure of the copolymer. The take-off angle used in these measurements was 90°, and hence the values reported here reflect the composition of approximately the upper ~11 nm of the material.[21] The data demonstrated a moderate enrichment of the surface layer with the fluorinated groups by a factor of 1.1 to 1.3, compared with the bulk composition for the statistical copolymers (see the right-hand column of Table 2). A more pronounced effect was observed for the block copolymers for which the composition at the surface was 30-50% higher than the average composition of the bulk polymer. This indicates that the assembly of fluorinated groups at the surface is conformationally frustrated for the statistical copolymers compared with the block copolymers, which are able to more readily present the fluorine-containing segments to the polymer-air interface.

Table 2 Composition of the surface determined by XPS and the bulk composition from the polymer structure.

Polymer	Bulk			XPS			XPS/ Bulk
	O (%)	C (%)	F (%)	O (%)	C (%)	F (%)	
poly(MMA$_{37}$-*block*-F3MA$_{11}$)	21.5	61.2	17.3	19	55	26	1.51
poly(MMA$_{33}$-*block*-F3MA$_{22}$)	18.2	56.4	25.5	15	45	39	1.54
poly(MMA$_{37}$-*block*-F3MA$_{26}$)	18.0	56.1	26.0	15	48	37	1.42
poly(MMA$_{33}$-*block*-F3MA$_{39}$)	16.1	53.4	30.5	12	47	40	1.31
poly(MMA$_{33}$-*block*-F3MA$_{49}$)	15.4	52.4	32.2	11	44	45	1.39
poly(MMA$_{82}$-*stat*-F3MA$_{18}$)	22.7	63.0	14.3	22	59	19	1.31
poly(MMA$_{69}$-*stat*-F3MA$_{21}$)	21.4	61.1	17.5	20	57	23	1.31
poly(MMA$_{58}$-*stat*-F3MA$_{20}$)	20.9	60.3	18.8	19	57	25	1.31
poly(MMA$_{32}$-*stat*-F3MA$_{34}$)	16.5	53.9	29.7	16	53	31	1.05
poly(MMA$_{15}$-*stat*-F3MA$_{48}$)	13.7	49.8	36.5	13	46	42	1.14

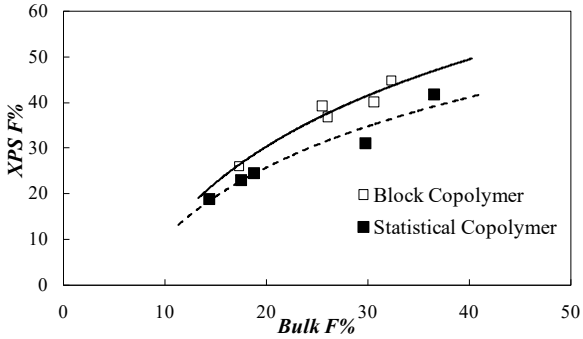

Figure 3 Fluorine content of the ~11 nm surface layer of the copolymer films determined by XPS as a function of the bulk composition expected from the structures of the copolymers.

A consequence of the localisation of the fluorinated segments at the polymer-air interface is a reduction in the surface energy. In this study the surface energy was determined from measurements of the contact angles that two liquids, water and diiodomethane, make with the polymer surface.[22] The dispersive, polar, and total surface energies are listed in Table 3, and the total surface energy (γ) is plotted as a function of composition of the copolymers in Figure 4. In all cases, and in particular for the block copolymers, the surface energy was dominated by the dispersive component, with minor contributions from the polar or Lewis acid component of the

surface energy. For the statistical copolymers, the contribution from the polar component decreases with increasing content of the fluoromonomer.

Table 3 Contact angles and surface energies of the two homopolymers and block and statistical copolymers of MMA and F3MA.

Polymer	Contact Angle (°)		Surface Energy (mJ/m^2)		
	Water	Diiodomethane	γ_D	γ_P	γ
PMMA	69.8	37.8	35.8	8.7	44.5
PF3MA	114.5	92.7	11.0	0.7	11.6
poly(MMA$_{37}$-*block*-F3MA$_{11}$)	108.9	91.5	11.0	1.7	12.6
poly(MMA$_{33}$-*block*-F3MA$_{22}$)	109.6	94.9	9.5	1.9	11.4
poly(MMA$_{37}$-*block*-F3MA$_{26}$)	110.7	95.6	9.3	1.7	11.0
poly(MMA$_{33}$-*block*-F3MA$_{39}$)	111.7	95.6	9.4	1.5	10.9
poly(MMA$_{33}$-*block*-F3MA$_{49}$)	112.4	96.2	9.2	1.4	10.6
poly(MMA$_{82}$-*stat*-F3MA$_{18}$)	93.6	75.5	17.5	4.2	21.7
poly(MMA$_{69}$-*stat*-F3MA$_{21}$)	96.5	79.0	15.9	3.7	19.6
poly(MMA$_{58}$-*stat*-F3MA$_{20}$)	98.6	79.3	16.0	3.0	19.0
poly(MMA$_{32}$-*stat*-F3MA$_{34}$)	104.9	86.1	13.2	2.0	15.2
poly(MMA$_{15}$-*stat*-F3MA$_{48}$)	109.5	93.7	10.0	1.8	11.8

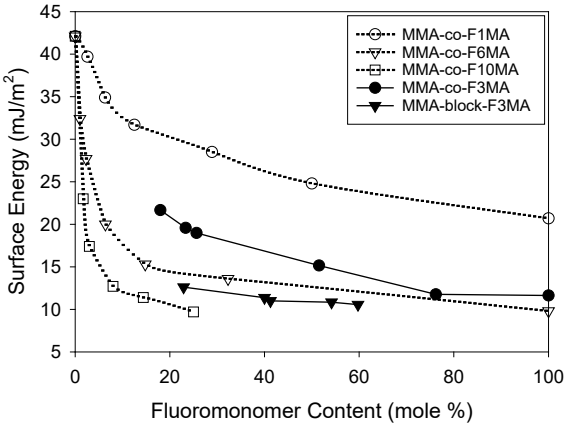

Figure 4 Surface energies of block and statistical copolymers of MMA and fluoromethacrylates, reported by van de Grampel et al.[8] (empty symbols) and measured here (full symbols) determined from measurements of contact angles. The lines are intend to be a guide to the eye.

A number of authors, most notably van de Grampel et al.,[8,23-25] have examined the effect of molecular parameters on the surface structure and surface free energies of copolymers of MMA with partly-fluorinated methacrylate monomers. In an early study, Tsibouklis et al.[26] reported that the surface energy of homopolymers of perfluoroalkyl methacrylates, obtained from measurements of contact angles, decreases with increasing length of the fluoroalkyl chain. Subsequently, Prathab and co-workers[27] used sequential molecular mechanics and molecular dynamics simulations of bulk amorphous and thin films of an homologous series of fluoroalkyl methacrylates and found a similar trend of decreasing surface energy with increasing length of the side chain. The results of the current study can be compared with those of van de Grampel who reported experimental surface energies of statistical copolymers of fluoroalkyl methacrylates and MMA. The fluoroalkyl methacrylates examined by them contained one, six or 10 fluorinated units, and were designated F1MA, F6MA and F10MA. In this study we have examined the properties of the previously unreported series of statistical copolymers of MMA and F3MA and compare these to a series of block copolymers prepared from the same monomers. van de Grampel reported that surface energies of statistical copolymers having compositions close to 25 mol% fluorinated monomer decrease continually from 28.5, 13.6 and 9.6 for F1MA-F10MA copolymers. The value reported here for statistical copolymers of MMA and F3MA of this approximate composition is 11.8 mJ/m^2, in good agreement with the trend reported by these authors.

In Figure 4 the surface energies of films of the statistical copolymers of F3MA and MMA are plotted as a function of the copolymer composition (filled circles). The data shows a decrease in surface energy from 44.5 mJ/m^2 for pure PMMA to 21.7 mJ/m^2 on inclusion of 18 mol% of F3MA. The surface energy then steadily decreases with increasing F3MA content to 11.6 mJ/m^2, for the homopolymer of F3MA. The data from van de Grampel et al.[8] for statistical copolymers F1MA, F6MA and F10MA with MMA have also been plotted as a comparison and similar trends can be observed as a function of fluoromonomer content. As expected, the F3MA curve also sits between the F1MA and F6MA curves. These results are consistent with the known tendency of fluorinated segments to preferentially segregate to the polymer-air interface. Both van de Grampel et al.[8] and Prathab and co-workers[27] reported self consistent field (SCF) calculations and molecular dynamics simulations of the phase structure of statistical copolymers of MMA with fluoromethacrylate monomers and were able to closely reproduce the experimental surface energies derived from the cohesive energy density calculated for the surface layer. Of relevance to this study, van de Grampel and colleagues[24] noted that the experimental surface energies decreased more rapidly than expected from the SCF calculations, and ascribed this to non-random placement of monomer units along the polymer chain. This is entirely reasonable given the likely large differences in reactivity ratios of the monomer pairs. We have previously demonstrated that trifluoroethyl methacrylate (F1MA) is incorporated at a slower rate compared with other methacrylate monomers during free radical polymerisation.[28] For example in our previous work we reported for the comonomer pair oligoethylene glycol methyl ether methacrylate (OEGMA 475) and F1MA are 2.46 and 0.22, respectively.[28] Unfortunately reactivity ratios and Q-e values for the monomer pair considered here have not been reported.

Figure 4 also includes the set of data from the block copolymers prepared in this work (solid inverted triangle symbols). It can be seen that the block copolymers consistently have a lower surface energy than the F3MA-based statistical copolymers and that the magnitude of the surface energy changes only 2 mJ/m^2, despite the fluoromonomer content varying almost 40 mole%. As noted above van de Grampel et al. considered the effects of differences in sequence distribution on the segregation behaviour of this class of copolymers, including block copolymers. They presented the results of SCF calculations that support a strong tendency of the fluoromethacrylate block to be preferentially localized at the polymer-air interface. However experimental verification of the results of their simulations was not provided. The data provided in this work and shown in Figure 4 confirms a more pronounced decrease in surface energy in block copolymer compared with the corresponding statistical copolymers.

Bulk phase structure of copolymers

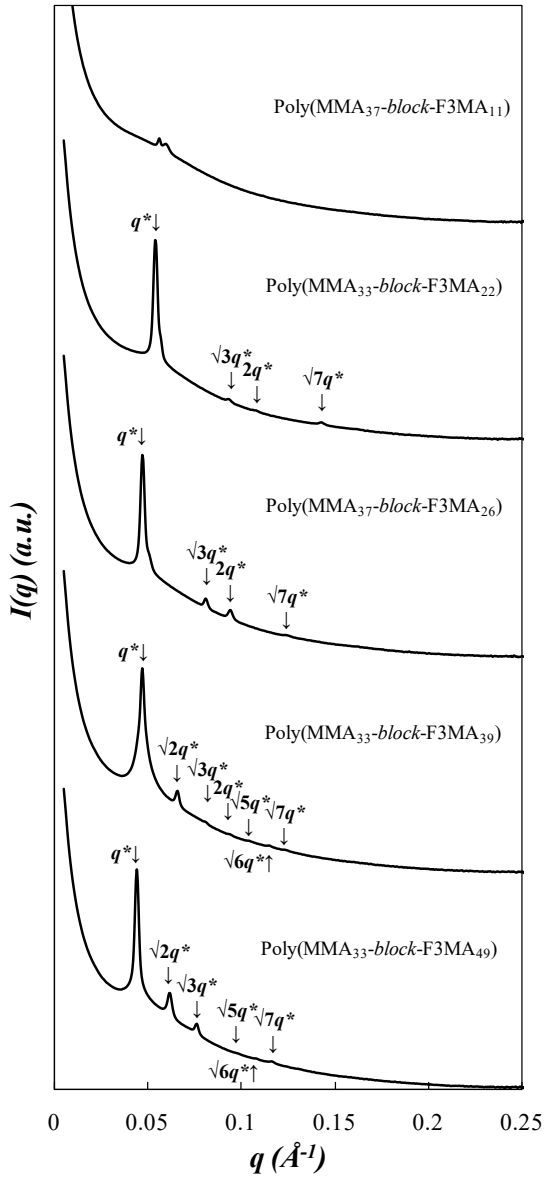

Figure 5 SAXS patterns of the block copolymer of MMA and F3MA after annealing at 150 °C for 2 h. The peak patterns are indicated with arrows and their respective positions. The upper X-axis shows the positions of higher order peaks in respect to the first and most intense peak, q*.

The phase structure of the polymers was examined by small-angle x-ray scattering (SAXS). The one-dimensional SAXS profiles for the five block copolymer samples are shown in Figure 5 and the Bragg peaks have been labelled with the assignments associated with the matching phase-separated morphology. The polymer with the highest content of MMA, poly(MMA_{37}-*block*-$F3MA_{11}$, the upper-most trace in Figure 5, shows relatively poor order, as evidenced by what appears to be a weak primary peak that is superimposed on a broader disordered peak. This is consistent with a morphology that contains both disordered and ordered phases separated regions [29]. We therefore conclude that this sample has a composition which places it close to the order-disorder phase boundary. The other four samples all exhibit sharp primary Bragg peaks as well as numerous higher-order peaks, indicating strong ordering of the phase separated domains. The relative spacings of the Bragg peaks allows assignment of the phase structure of the block copolymers, and the results, and long periods for each phase, are summarized in Table 4. Explicitly the copolymers poly(MMA_{33}-*block*-$F3MA_{22}$) and poly(MMA_{37}-*block*-$F3MA_{26}$) show Bragg peaks at relative peak positions q/q^*equal to 1: √3: 2: √7, indicative of hexagonal morphology. The lower two traces in Figure 5 show peaks at 1: √2: √3: √4: √5: etc., indicative of a body-centred cubic spherical morphology. The full details of the domain sizes calculated for these polymers can be found in the Supporting Information.

As mentioned above, the polymer with the highest content of MMA, poly(MMA_{37}-*block*-$F3MA_{11}$), shows weak phase structure, and hence we conclude that its composition lies close to order-disorder phase boundary. The volume fraction of the MMA block in this polymer, calculated assuming a density of 1.48 g/cm^3 for the F3MA block, is 0.61. For symmetrical block copolymers the phase boundary will be found for polymers with a product of the Flory-Huggins polymer-polymer interaction parameter (χ) and the total degree of polymerisation (N) being χN equal to 10.5.[30] Under these assumptions, an approximate value of χ for PMMA and

PF3MA was calculated to be 0.22. This allows a value of the solubility parameter (δ_2) for PF3MA equal to 17.2 to be calculated assuming a value of δ_2 for PMMA of 19.5.[31] Very few reports exist in the literature of the solubility parameters of fluorinated methacrylate polymers, apart from several studies using inverse gas chromatography by Papadopoulou and colleagues.[32-35] In addition to that work, we have previously[36] used the Van Krevelen group contribution method to calculate a solubility parameter (δ_2) for PF1MA of 17.1 $(MPa)^{0.5}$, in good agreement with the value obtained by extrapolating the data of Papadopoulou et al.[35] to room temperature. Using the same approach for the current system, we obtain a value of δ_2 for PF3MA equal to 16.7, close to the experimental value of 17.2. Finally the value of interaction parameter of 0.22 allows calculation of the expected morphologies of the other four block copolymers, and these are in excellent agreement with the structures confirmed by SAXS measurement (Table 4).

These results clearly demonstrate the ability of the block copolymers prepared in this study to undergo phase separation in the bulk. It should be noted however, that when the polymers are confined in thin films the influence of interactions at the silicon-polymer and polymer-air interfaces will also influence the morphology of the films. [37] Considering the ability of the block copolymers to phase separate and the very low surface energies that are almost independent of fluorine content in the top 11 nm, it can be inferred that the block copolymers are presenting a phase separated layer at the polymer-air interface. This is consistent with other reports, including a self-consistent field study of the effect of confinement on the interface of block copolymers by Yang et al., who demonstrated the formation of parallel lamellar phases at the interface in many cases.[37] To compare this with the statistical copolymers (refer to Figure 4), it is clear that the surface energy decreases with decreasing fluorine content in the top 11 nm which is probed by XPS. This can be attributed to the statistical sequence of the copolymers, which introduces conformational frustrations that prevent a proportion of the fluorine-containing repeat units from being presented at the polymer-air interface. A key outcome of this study is that block copolymers with a fluorinated block are significantly more effective at reducing the surface energy of films than statistical copolymers prepared from the same monomers. In addition, they can be more effective than statistical copolymers prepared with monomers with longer fluoroalkyl units. For example, the F3MA block copolymers prepared here exhibited lower surface energies than the F6MA statistical copolymers reported by van de Grampel,[8] despite a lower overall fluorine content. In addition, the apparent formation of a surface layer of the fluorinated block also results in surface energies that are almost invariant ($\triangle\gamma$ = 2 mJ/m^2) over a fluoromonomer composition that varies by almost 40%. This shows that the block length can be significantly reduced without paying a significant penalty in terms of increased surface energy. These findings have particular environmental significance because alkyl chains with extended fluorination are increasingly being implicated as persistent organic pollutants. For example, C8-C15 perfluoroalkyl chains have been shown to be persistent in the environment and undergo bioaccumulation in various aquatic species.[5,6] On the other hand, shorter perfluorinated alkyl chains have a much lower degree of bioconcentration.[7] In addition shorter blocks can be used to achieve almost the same surface properties. Hence, the block copolymers presented here may provide a more environmentally-acceptable avenue to fabricate surfaces with ultra-low surface energies.

Table 4 Phase assignments and long periods for the block copolymers. The phase structure of poly(MMA_{37}-*block*-$F3MA_{11}$) is weakly defined and cannot be assigned. Calculation of the SAXS lattice parameters is described in Supporting Information Figure S3.

Block Copolymer	Phase Type	Long Period (nm)
poly(MMA_{37}-*block*-$F3MA_{11}$)	--	11.2
poly(MMA_{33}-*block*-$F3MA_{22}$)	Hexagonal	11.7
poly(MMA_{37}-*block*-$F3MA_{26}$)	Hexagonal	13.4
poly(MMA_{33}-*block*-$F3MA_{39}$)	Spherical (BCC)	13.4
poly(MMA_{33}-*block*-$F3MA_{49}$)	Spherical (BCC)	14.3

CONCLUSIONS

A range of novel block and statistical copolymers of MMA and F3MA have been prepared by RAFT polymerisation and their surface and bulk properties examined in detail. A methacrylate having a short (n=3) fluoroalkyl side chain was chosen because of increasing limits on use of longer fluorocarbons due to environmental concerns. The phase separation indicated by these results was confirmed by synchrotron small-angle x-ray scattering measurements of the bulk phase structure. A range of morphologies from spherical to cylindrical were confirmed, consistent with the expected behaviour for block copolymers. Furthermore, the observation of weak ordering in one of the compositions has allow the estimation of an interaction parameter and hence the first report of the solubility parameter of polymers of F3MA. The surface energies of the copolymers are diminished by the incorporation of the fluoromethacrylate, indicative of localisation of those repeat units at the polymer-air interface. The decrease in surface energy is consistent with the size of the fluoromonomer side chain, and in line with previously reported values for other members of this family of statistical copolymers. The block copolymers consistently show a more efficient reduction in surface energy compared to statistical copolymers of made from the same monomers which was attributed to formation of a surface layer of the fluorinated block. The surface energies were also comparable to statistical copolymers prepared from monomers containing longer perfluoro chains. This demonstrates that the materials presented here may be a more environmentally acceptable alternative to polymers containing long perfluoro chains, without sacrificing surface properties.

ACKNOWLEDGEMENTS

The authors would like to acknowledge Dr Hui Peng's University of Queensland Postdoctoral Research Fellowship for Women, the Australian Research Council for funding (CE140100036, DP130103774, DP0987407, DP110104299, FT100100721 and DP140103118) and Australian National Fabrication Facility, Queensland Node for access to some items of equipment. SAXS experiments were undertaken on the SAXS/WAXS beam-line at the Australian Synchrotron, Victoria, Australia.

REFERENCES AND NOTES

1. E. Lindner. *Biofouling* **1992**, *6*, 193-205.
2. D. L. Schmidt, R. F. Brady, K. Lam, D. C. Schmidt, M. K. Chaudhury. *Langmuir* **2004**, *20*, 2830-2836.
3. J. C. Yarbrough, J. P. Rolland, J. M. DeSimone, M. E. Callow, J. A. Finlay, J. A. Callow. *Macromolecules* **2006**, *39*, 2521-2528.
4. M. D. Dimitriou, Z. Zhou, H.-S. Yoo, K. L. Killops, J. A. Finlay, G. Cone, H. S. Sundaram, N. A. Lynd, K. P. Barteau, L. M. Campos, D. A. Fischer, M. E. Callow, J. A. Callow, C. K. Ober, C. J. Hawker, E. J. Kramer. *Langmuir* **2011**, *27*, 13762-13772.

5. K. Kannan, S. Corsolini, J. Falandysz, G. Oehme, S. Focardi, J. P. Giesy. *Environmental Science & Technology* **2002**, *36*, 3210-3216.
6. J. W. Martin, M. M. Smithwick, B. M. Braune, P. F. Hoekstra, D. C. G. Muir, S. A. Mabury. *Environmental Science & Technology* **2004**, *38*, 373-380.
7. J. W. Martin, S. A. Mabury, K. R. Solomon, D. C. G. Muir. *Environmental Toxicology and Chemistry* **2003**, *22*, 196-204.
8. R. D. van de Grampel, W. Ming, A. Gildenpfennig, W. J. H. van Gennip, J. Laven, J. W. Niemantsverdriet, H. H. Brongersma, G. de With, R. van der Linde. *Langmuir* **2004**, *20*, 6344-6351.
9. M. A. Hillmyer, T. P. Lodge. *J. Polym. Sci., Part A: Polym. Chem.* **2001**, *40*, 1-8.
10. M. A. Hillmyer, T. P. Lodge. *Journal of Polymer Science Part A: Polymer Chemistry* **2002**, *40*, 1-8.
11. Y. Ren, T. P. Lodge, M. A. Hillmyer. *Macromolecules* **2002**, *35*, 3889-3894.
12. H. Yokoyama, K. Tanaka, A. Takahara, T. Kajiyama, K. Sugiyama, A. Hirao. *Macromolecules* **2004**, *37*, 939-945.
13. H. Yokoyama, K. Sugiyama. *Langmuir* **2004**, *20*, 10001-10006.
14. S. H. Thang, Y. K. Chong, R. T. A. Mayadunne, G. Moad, E. Rizzardo. *Tetrahedron Letters* **1999**, *40*, 2435-2438.
15. S. Perrier, P. Takolpuckdee, C. A. Mars. *Macromolecules* **2005**, *38*, 2033-2036.
16. A. S. Brar, S. Hooda, R. Kumar. *Journal of Polymer Science Part A: Polymer Chemistry* **2003**, *41*, 313-326.
17. S. Krishnan, R. Ayothi, A. Hexemer, J. A. Finlay, K. E. Sohn, R. Perry, C. K. Ober, E. J. Kramer, M. E. Callow, J. A. Callow, D. A. Fischer. *Langmuir* **2006**, *22*, 5075-5086.
18. S. Krishnan, R. J. Ward, A. Hexemer, K. E. Sohn, K. L. Lee, E. R. Angert, D. A. Fischer, E. J. Kramer, C. K. Ober. *Langmuir* **2006**, *22*, 11255-11266.
19. H. Li, Z. B. Zhang, C. P. Hu, S. S. Wu, S. K. Ying. *European Polymer Journal* **2004**, *40*, 2195-2201.
20. H. Ni, J. Gao, X. Li, Y. Hu, D. Yan, X. Ye, X. Wang. *Journal of Colloid and Interface Science* **2012**, *365*, 260-267.
21. S. Tanuma, C. J. Powell, D. R. Penn. *Surface and Interface Analysis* **1994**, *21*, 165-176.
22. D. K. Owens, R. C. Wendt. *Journal of Applied Polymer Science* **1969**, *13*, 1741-1747.
23. R. D. van de Grampel, W. Ming, A. Gildenpfennig, W. J. H. van Gennip, M. J. Krupers, J. Laven, J. W. Niemantsverdriet, H. H. Brongersma, R. van der Linde. *Progress in Organic Coatings* **2002**, *45*, 273-279.
24. R. D. van de Grampel, W. Ming, J. Laven, R. van der Linde, F. A. M. Leermakers. *Macromolecules* **2002**, *35*, 5670-5680.
25. R. D. van de Grampel, W. H. Ming, J. Laven, R. van der Linde, F. A. M. Leermakers. *Polymer* **2007**, *48*, 3877-3882.
26. J. Tsibouklis, P. Graham, P. J. Eaton, J. R. Smith, T. G. Nevell, J. D. Smart, R. J. Ewen. *Macromolecules* **2000**, *33*, 8460-8465.
27. B. Prathab, T. M. Aminabhavi, R. Parthasarathi, P. Manikandan, V. Subramanian. *Polymer* **2006**, *47*, 6914-6924.
28. C. Zhang, H. Peng, A. K. Whittaker. *Journal of Polymer Science Part A: Polymer Chemistry* **2014**, *52*, 2375-2385.
29. J. L. Thelen, A. A. Teran, X. Wang, B. A. Garetz, I. Nakamura, Z.-G. Wang, N. P. Balsara. *Macromolecules (Washington, DC, U. S.)* **2014**, *47*, 2666-2673.
30. L. Leibler. *Macromolecules* **1980**, *13*, 1602-1617.
31. J. Brandup, E. H. Immergut, E. A. Grulke, Eds. Polymer Handbook; Wiley, **2003**.
32. S. K. Papadopoulou, G. Dritsas, I. Karapanagiotis, I. Zuburtikudis, C. Panayiotou. *European Polymer Journal* **2010**, *46*, 202-208.
33. S. K. Papadopoulou, I. Karapanagiotis, I. Zuburtikudis, C. Panayiotou. *Journal of Polymer Science Part B: Polymer Physics* **2010**, *48*, 1826-1833.
34. S. K. Papadopoulou, C. Panayiotou. *Journal of Chromatography A* **2012**, *1229*, 230-236.
35. S. K. Papadopoulou, C. Panayiotou. *Journal of Chromatography A* **2014**, *1324*, 207-214.
36. H. Peng, K. J. Thurecht, I. Blakey, E. Taran, A. K. Whittaker. *Macromolecules* **2012**, *45*, 8681-8690.
37. Y. Yang, F. Qiu, H. Zhang, Y. Yang. *Polymer* **2006**, *47*, 2205-2216.